Electronic Supplementary Material (ESI) for ChemComm.

Nanohybrids from Nanotubular J-Aggregates and Transparent Silica Nanoshells

Yan Qiao,[a,b,c*] *Frank Polzer,*[a,d] *Holm Kirmse,*[a] *Stefan Kirstein,*[a*] *and Jürgen P. Rabe*[a,b]

[a] Department of Physics, Humboldt-Universität zu Berlin, Newtonstr 15, 12489 Berlin, Germany.

[b] IRIS Adlershof, Humboldt-Universität zu Berlin, Zum Großen Windkanal 6, 12489 Berlin, Germany.

[c] present address: Centre for Protolife Research and Centre for Organized Matter Chemistry, School of Chemistry, University of Bristol, Bristol BS8 1TS, United Kingdom.

[d] present address: Materials Science & Engineering, University of Delaware, Newark, DE 19716, USA.

Supporting Information

1. Materials and methods

Preparation of tubular J-aggregates. Double-walled J-aggregate nanotubes were prepared in water/methanol (9:1, v/v). Stock solution of C8S3 (2.92 mM) was prepared by directly dissolving C8S3 powder (FEW Chemicals, Germany) in methanol (⩾99.9% GC, Sigma-Aldrich). Then 130 μL of the C8S3 stock solution was added to 500μL of ultrapure H_2O followed by thorough vortex to ensure complete mixing. An immediate color change of the solution (from orange to deep pink) was observed, indicating the formation of tubular J-aggregates. The solution was stored in the dark for 24 h before adding an additional 500 μL of ultrapure H_2O, which gave a final concentration of 0.336 mM. Fresh J-aggregate solutions were stored in the dark and used within three days after preparation.

Preparation of silica nanoshell on the C8S3 J-aggregate. For the helical silica shell synthesis, typically, 2 μL of 3-aminopropyltriethoxysilane (APTES, sigma, 99%) methanol solution (v/v = 1:49) and 15 μL tetraethoxysilane (TEOS, sigma, 99%) methanol solution (v/v = 1:49) were added to 250 μL of J-aggregate solution. The mixture was vortexed to ensure complete mixing and incubate for 24 hours to finish the silanization reaction before measurement. To synthesize silica in the absence of APTES as a control experiment, 17 μL of TEOS in methanol solution (v/v = 1:49) was added to a 250 μL of J-aggregate solution. All the experiments were finished under red light and the samples were stored for 24 h in dark to protect from photobleaching.

Absorption spectroscopy. Absorption spectra of the solution were taken with a double-beam UV-vis spectrometer (Shimadzu UV-2101PC, Duisberg, Germany) in a 0.2 mm, 1.0 mm, or 10.0 mm demountable quartz cell (Hellma GmbH, Germany). The UV sample prepared by growth of the silica nanoshell *in situ* inside of the cuvettes which means the hybrids were moved to the cuvettes immediately after the addition of silica precursor and stored for 24 hours before measurement.

Fluorescence spectroscopy. Fluorescence spectra were taken on a fluorescence spectrometer (JASCO FP 6500) in quartz cells (Hellma GmbH, Germany) with the path length of 0.2 mm, 1.0 mm, or 10.0 mm. The fluorometer came with built-in light-source (Xe-lamp UXL-159, 150W), two grating-monochromators with variable slit-width and detector. The photobleaching experiments were conducted at a wavelength of 500 nm (slit width = 10 nm).

Cryogenic transmission electron microscopy (Cryo-TEM). Droplets of the solution (5 μL) were applied to carbon film (1 μm hole diameter) covered 200 mesh grids (R1/4 batch of Quantifoil Micro Tools GmbH, Jena, Germany), which had been hydrophilized before use by plasma process. Supernatant fluid was removed by Vitrobot Mark Ⅳ (FEI company, Eindhoven, Netherlands) until an ultrathin layer of the sample solution was obtained spanning the holes of the carbon film. The samples were immediately vitrified by propelling the grids into liquid ethane at its freezing point (90 K). Frozen samples were transferred into a JEOL JEM2100 (JEOL, Eching, Germany) using a Gatan 914 high-tilt cryo-transfer holder and Gatan work station (Gatan, Munuch, Germany). Microscopy was carried out at a 94 K sample temperature using the microscope's low-dose protocol at an accelerating voltage of 200 kV (LaB6-illumination). The defocus was chosen to be approx 2 μm to create sufficient phase contrast for imaging. Image analysis was performed with Image J software[1].

High Resolution Transmission Electron Microscopy (HR-TEM). High resolution transmission electron microscopy (TEM) was performed with a JEOL 2010F operating at 200 kV. Droplets of the sample (5 μL) were applied to carbon film coated 200 mesh grids (Quantifoil Micro Tools GmbH, Jena, Germany), which had been hydrophilized before use by simply storing the grids over a water bath for a day. The excess fluid was removed with a filter paper to form an ultra-thin layer on the carbon film. Image analysis was performed with Image J software[1].

2. Sketch and spectra of C8S3 J-aggregates

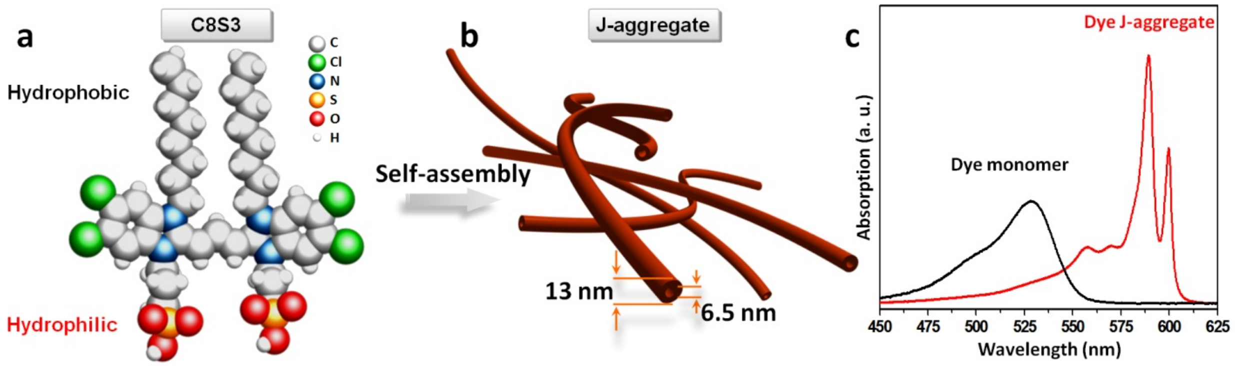

Figure S1. Sketch of molecular self-assembly into J-aggregates. (a) Molecular structure of amphiphilic cyanine dye C8S3; (b) sketch of nanotublular J-aggregates; (c) absorption spectra of C8S3 monomer (black) and J-aggregate (red) solution, in which J-aggregates exhibit narrow and red-shifted absorption peaks relative to monomers.

3. TEM image of silica nanoshell coated J-aggregate hybrids

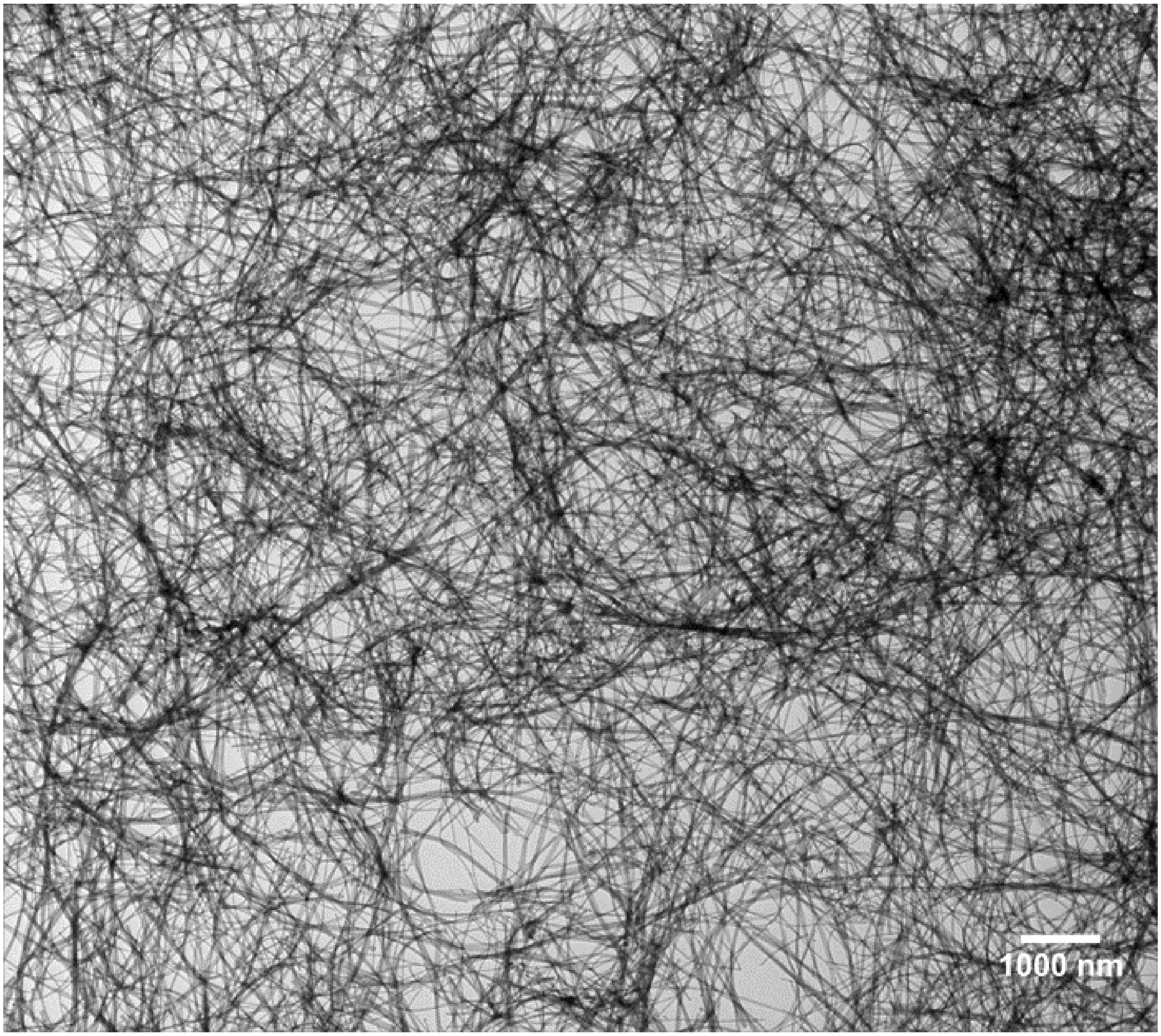

Figure S2. TEM image of silica nanoshell coated J-aggregate nanohybrids. The image shows tubular nanohybrids are several micrometers long.

4. HRTEM image of silica nanoshell coated J-aggregate hybrids

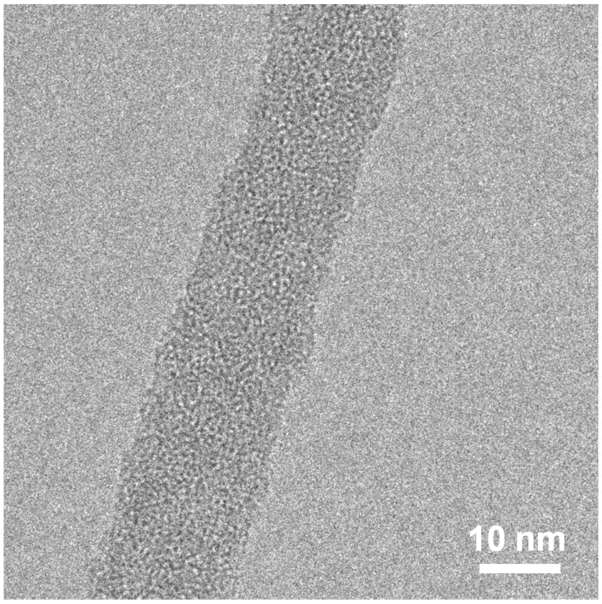

Figure S3. HR-TEM image of the as-prepared silica nanoshell-coated J-aggregate showing porous porous structure. In contrast to the cryo-TEM images shown in Figs. S5 and S6, this image was obtained from a sample that was dried on the supporting film of the TEM grid. Due to the drying process the helical superstructure seems to be lost.

5. EDXS analysis of silica nanoshell coated J-aggregate hybrids

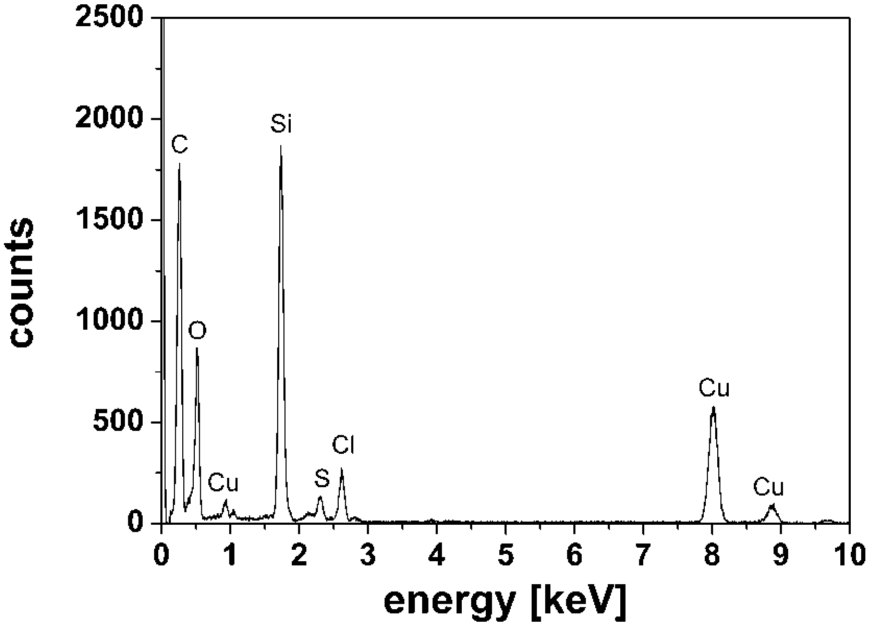

Figure S4. EDXS analysis of the as-prepared silica nanoshell-coated J-aggregate nanohybrids confirms the presence of Si and S elements.

6. Magnified cryo-TEM image of Fig. 1a

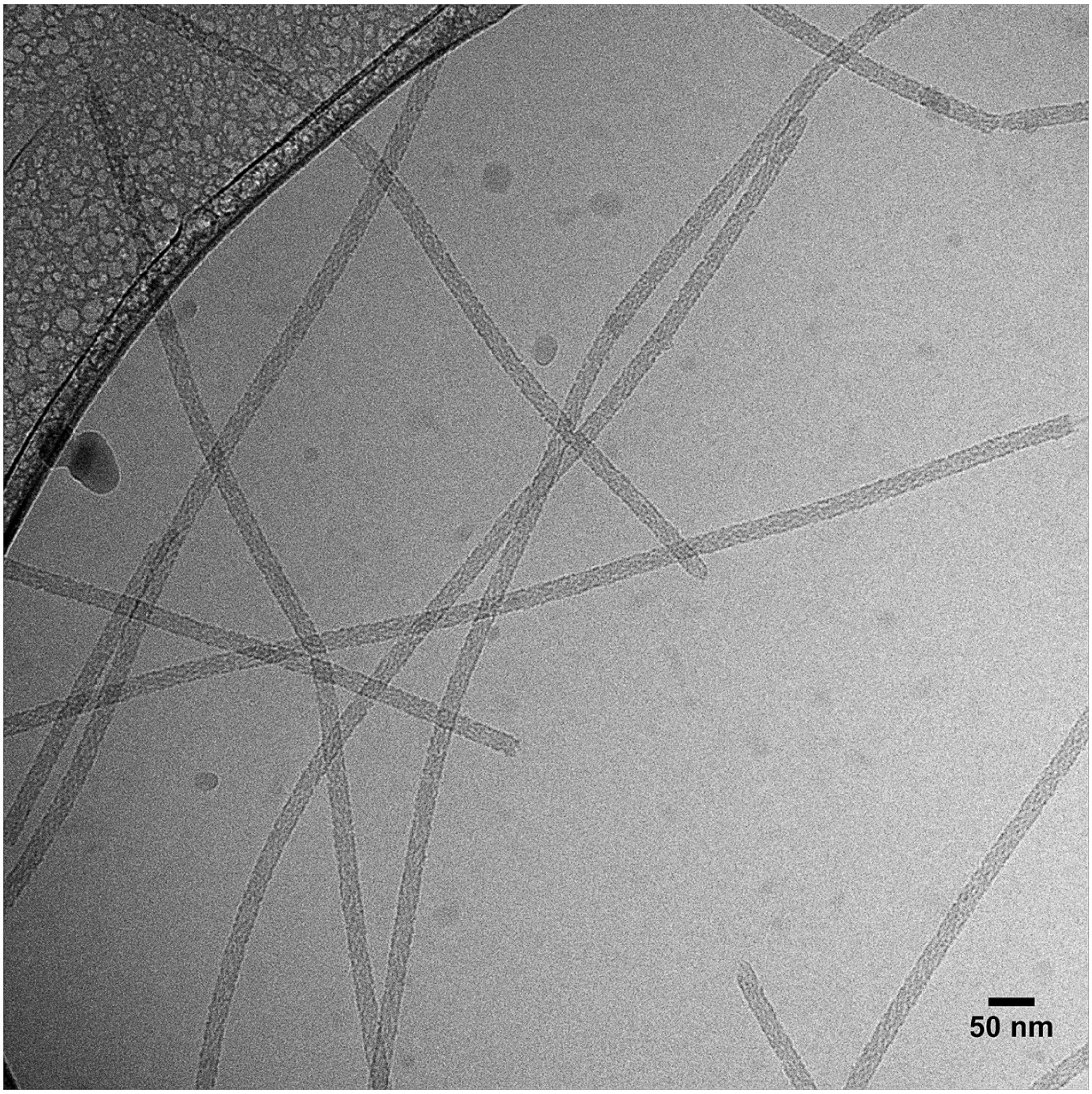

Figure S5. Magnified cryo-TEM image of silica coated J-aggregates as presented Fig. 1a. The helical structures can be observed on most of the nanohybrids.

7. Sketch of electrostatically driven silication of tubular J-aggregate

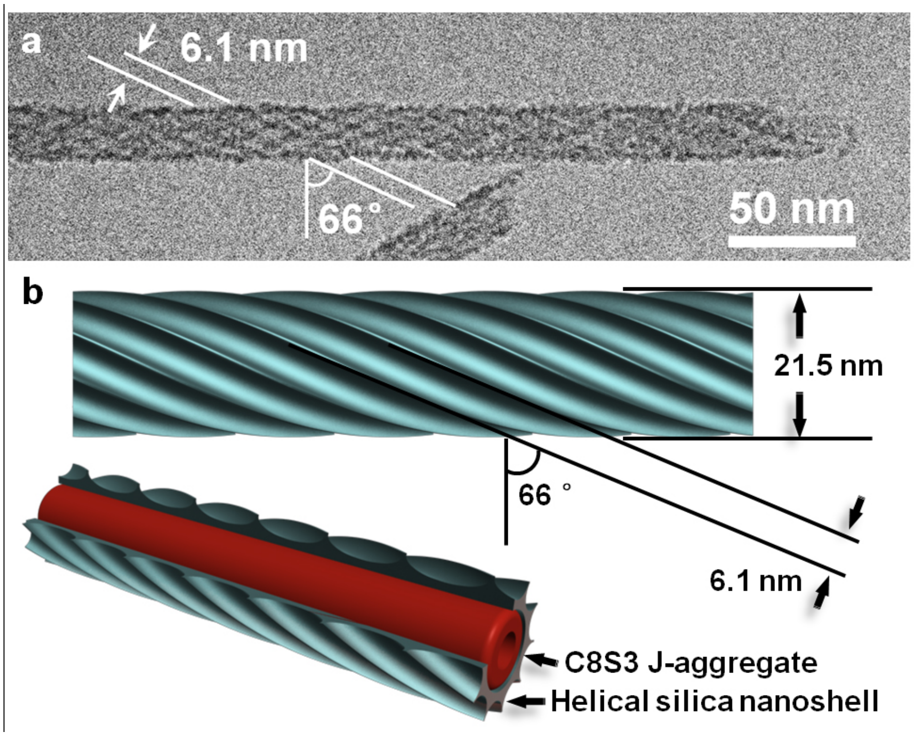

Figure S6. (a) Cryo-TEM image of silica nanoshell coated J-aggregates with detailed analysis of the superstructure. (b) 3D model of the surface and cross-section of silica coated J-aggregates exhibiting the parameters of helical structures.

8. Sketch of electrostatically driven silication of tubular J-aggregate

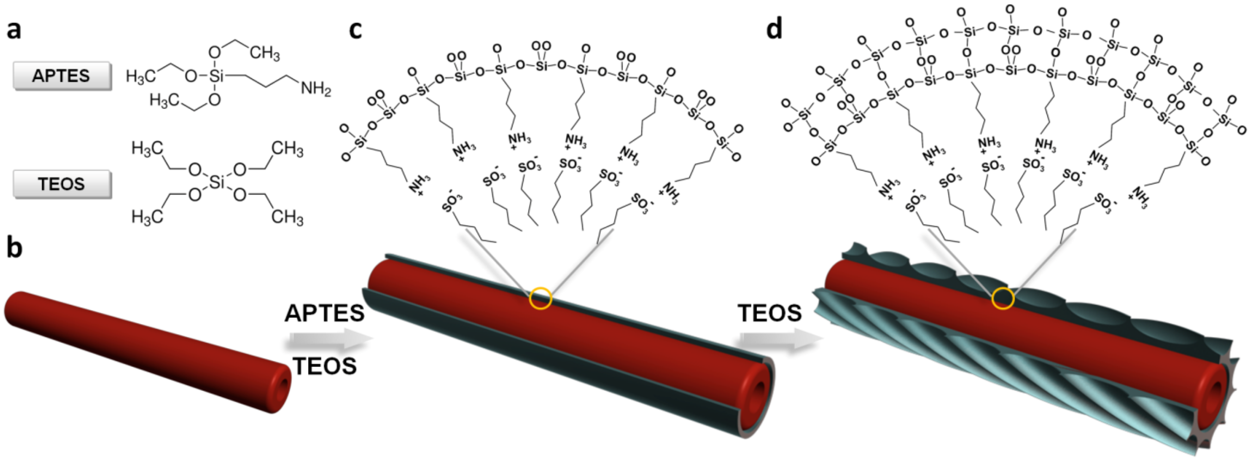

Figure S7. Sketch of electrostatically driven silication of tubular J-aggregate. (a) Molecular structures of the constituents: APTES, and TEOS; (b) sketch of J-aggregate nanotube, (c) electrostatic adsorption of APTES on J-aggregates; (d) condensation of TEOS on J-aggregate nanotubes.

9. Structural variation of nanohybrids by changing the reaction parameters

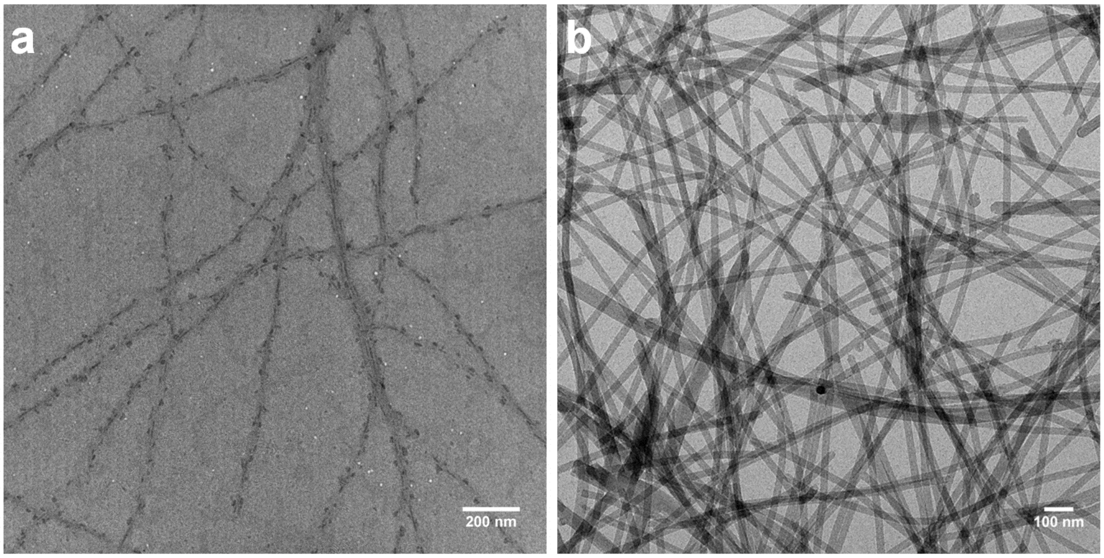

Figure S8. (a) TEM image of J-aggregates coated by discrete silica nanoparticles prepared by using TEOS alone as a precursor. The formation of discrete silica nanoparticles instead of silica ribbons was due to the absence of APTES that facilitates TEOS intermediates to bind evenly on the J-aggregate nanotube. The density of silica nanoparticles is low because the condensation of silica on the surface of J-aggregates is not favourable without APTES. (b) TEM images of silica coated J-aggregates prepared from the standard method, except that TEOS was added before APTES.

10. Measurement of fluorescence quantum yields of J-aggregate with and without silica shell

The fluorescence quantum yield (*Q*) is obtained using the comparative method of Williams *et al.*, which involves the use of well characterized standard fluorophore with known *Q* values. The quantum yield of the test sample is calculated using:

$$Q_X = Q_{ST}\left(\frac{I_X}{I_{ST}}\right)\left(\frac{OD_{ST}}{OD_X}\right)\left(\frac{\eta_X^2}{\eta_{ST}^2}\right)$$

Where the subscripts ST and X denote standard and test respectively, *Q* is the fluorescence quantum yield, *I* is the integrated fluorescence intensity, *η* is the refractive index, and *OD* is the optical density. In this work, a series of solutions were prepared with optical densities between 0.1 and 0.01, and a more accurate method was used to determine *Q* by the following formula:

$$Q_X = Q_{ST}\left(\frac{Grad_X}{Grad_{ST}}\right)\left(\frac{\eta_X^2}{\eta_{ST}^2}\right)$$

where *Grad* is the gradient obtained from the plot of integrated fluorescence intensity *I* versus the absorbance. Fluorescein in 0.1 M NaOH solution (*Q* = 95%)[2] Rhodamine B (*Q* = 31%)[3] was used as a standard sample for J-aggregate. All the fluorescence spectra were recorded with constant slit widths. The obtained quantum yields of J-aggregate with and without silica shell were 8%, and 6%, respectively.

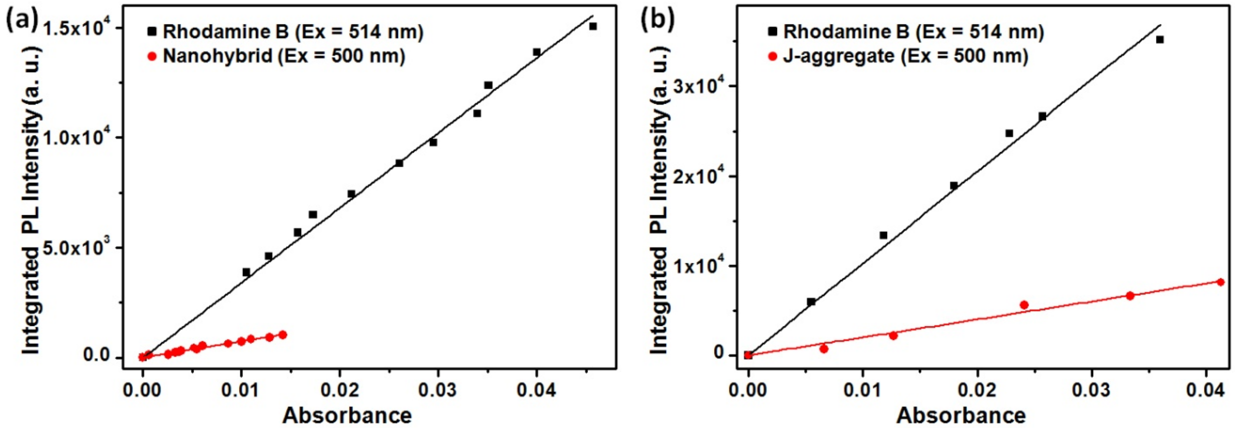

Figure S9. Linear plots of the measured absorption and integrated fluorescence intensity of: (a) rhodamine B and C8S3 J-aggregate; (b) rhodamine B and silica nanoshell-coated C8S3 J-aggregate.

11. Adjustable thickness of the silica nanoshell by varying the concentration of the silica precursor

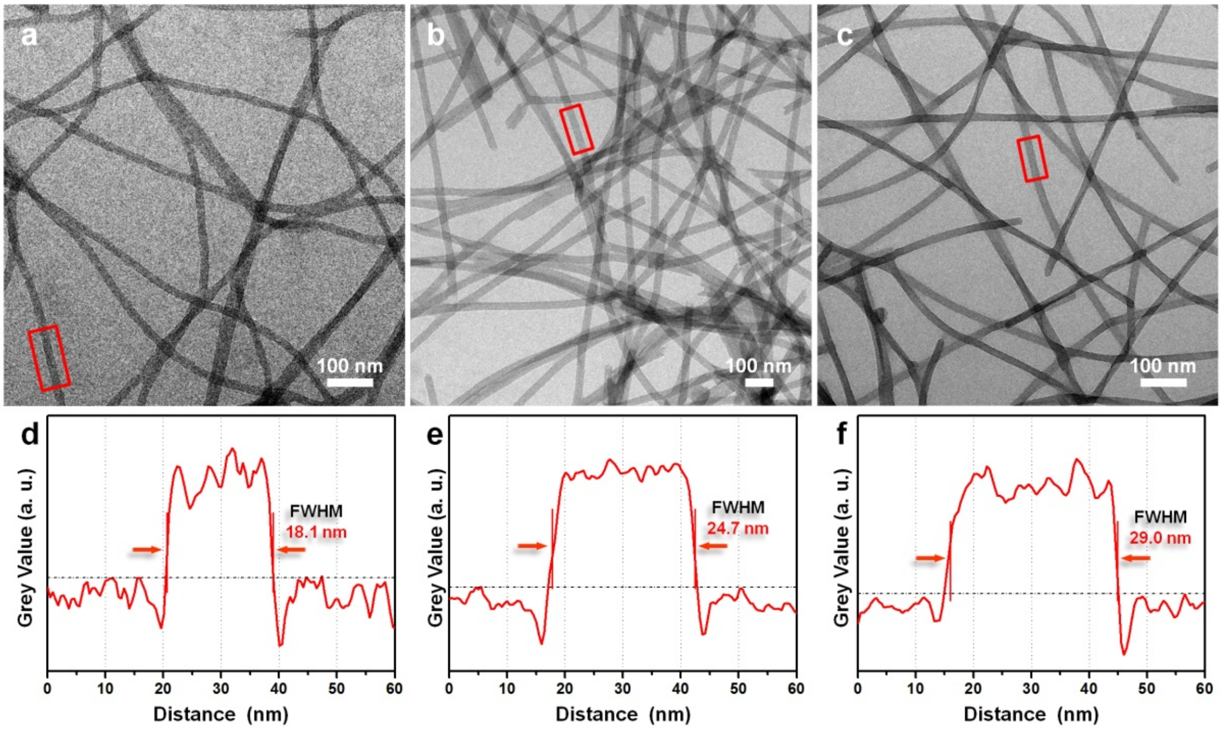

Figure S10. TEM images (a-c) and line scans (d-f) of silica coated nanohybrids prepared with different ATPES/TEOS concentrations. (a, d) 0.684 mM / 3.58 mM; (b, e) 0.684 mM / 10.7 mM and (c, f) 0.684 mM / 14.3 mM. When TEOS concentration increases, the thickness of silica shell increases while the helical patterns are not observed. This is possibly because the overgrowth of silica weakens the chiral features of the silica surface. Some bundled nanohybrids are also observed at high APTES/TEOS concentrations.

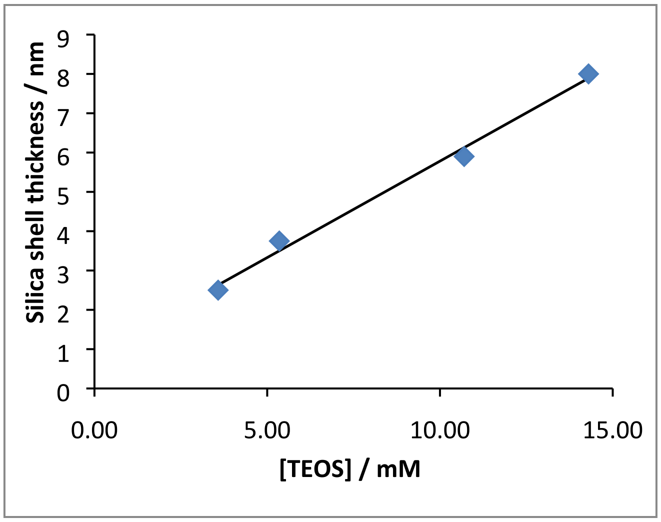

Figure S11. Plot of silica shell thickness versus concentration of TEOS. The shell thickness was calculated from the FWHM values of the total diameter of the J-aggregate/silica hybrid (as shown in Fig S6), by subtracting 13 nm for the pure J-aggregates, and division by two. The linear trend line of the silica thickness does not necessarily fit for TEOS concentration below 3.58 mM or above 14.8 mM.

12. Thermo stability of silica coated J-aggregate

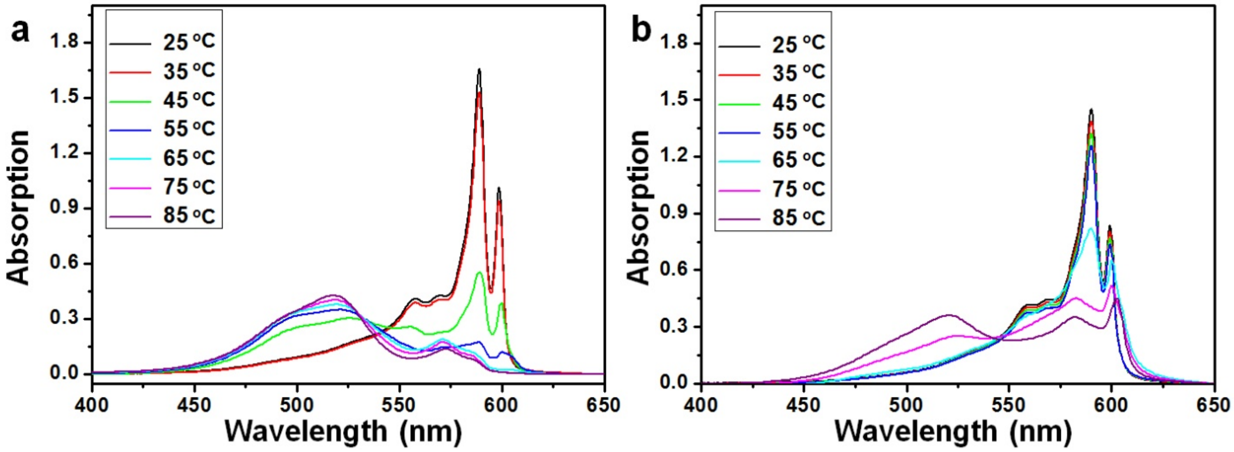

Figure S12. UV/vis absorption of (a) J-aggregates and (b) nanohybrids at different temperatures. J-aggregates were stable up to 35 °C, and started to disassemble at 45 °C. Nanohybrids were stable even at 55 °C, and started to disassemble into the C8S3 monomer at 65 °C.

13. Stability of silica coated J-aggregate against metal ions

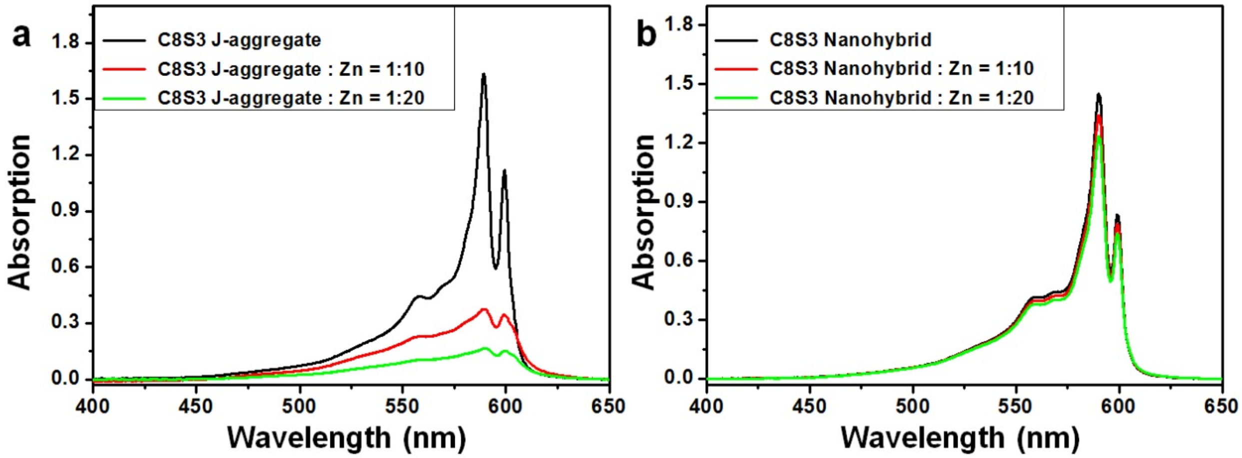

Figure S13. UV/vis absorption of (a) J-aggregates and (b) nanohybrids in the presence of $Zn(NO_3)_2$ at 3.36 mM (10 times of C8S3 concentration) and 6.72 mM (20 times of C8S3 concentration).

14. Preliminary photo-bleaching experiments

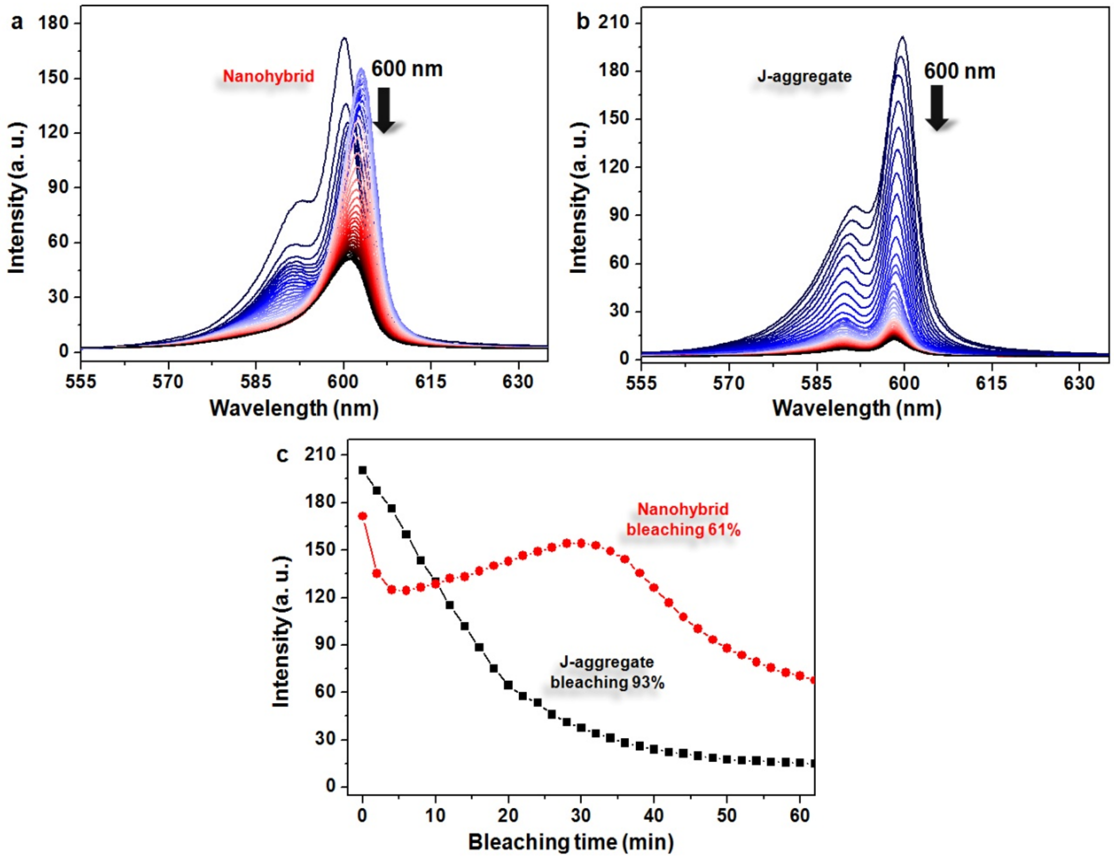

Figure S14. PL spectra of nanohybrids (a) and J-aggregates (b) recorded under radiation with Xe lamp (from fluorescence spectrometer); spectra were taken at time intervals of 2 min (λ_{ex}= 500 nm). (c) PL intensities (600 nm) of nanohybrids and J-aggregate versus photo bleaching time. The photo bleaching was conducted by irradiating the sample with the Xe lamp on fluorescence spectrometer.

References

1 W. S. Rasband, ImageJ, http://imagej.nih.gov/ij/, 1997-2012.

2 J. R. Lakowicz, *Principles of Fluorescence Spectroscopy*, Kluwer Academic/Plenum Publishers, New York, London, Moscow, Dordrecht, 1999.

3 D. Magde, G. E. Rojas and P. G. Seybold, *Photochem. Photobiol.*, 1999, **70**, 737-744.